

# Bond cutting in Cs-doped tris(8-hydroxyquinoline) aluminium

Hsin-Han Lee,<sup>a</sup> J. Hwang,<sup>a\*</sup> Tun-Wen Pi,<sup>b</sup> Y.-C. Wang,<sup>c</sup> W.-J. Lin<sup>c</sup> and C.-P. Cheng<sup>c</sup>

<sup>a</sup>Department of Materials Science and Engineering, National Tsing Hua University, Hsinchu 30013, Taiwan, <sup>b</sup>National Synchrotron Radiation Research Center, Hsinchu 30076, Taiwan, and <sup>c</sup>Department of Applied Physics, National Chiayi University, Chiayi 60004, Taiwan.  
E-mail: jch@mx.nthu.edu.tw

A series of Cs 4*d* and Al 2*p* spectra associated with valence-band and cut-off spectra have been used to characterize the interaction between caesium and tris(8-hydroxyquinoline) aluminium (Alq<sub>3</sub>) molecules in a Cs-doped Alq<sub>3</sub> layer. The Cs 4*d* and Al 2*p* spectra were tuned to be very surface sensitive by selecting a photon energy of 120 eV at the National Synchrotron Radiation Research Center, Taiwan. A critical Cs concentration exists, above which a new Al 2*p* signal appears next to the Al 2*p* peak of Alq<sub>3</sub> in the lower binding-energy side. The Al 2*p* signal was analyzed and assigned as being contributed from a mixture of Alq<sub>2</sub>, Alq and Al. Experimental data supported the observation that bond cutting of Alq<sub>3</sub> by the doped Cs atoms occurred at high Cs doping concentration.

**Keywords:** tris(8-hydroxyquinoline) aluminium; Cs doping; bond cutting; interface; photoemission.

## 1. Introduction

Doping in organic materials has attracted attention in the past years owing to the improvement in the performance of organic light-emitting devices (OLEDs) (Tang *et al.*, 1989; Shi & Tang, 1997). A metal-doped organic layer is usually formed by depositing a metal layer between the electron transport layer [tris(8-hydroxyquinoline) aluminium (Alq<sub>3</sub>)] and a cathode material Al. A common metal-doped organic layer used in an OLED device is the Li-doped Alq<sub>3</sub> layer near the cathode interface (Haskal *et al.*, 1997; Kido *et al.*, 1993; Kido & Matsumoto, 1998). Kido & Matsumoto (1998) demonstrated that a Li-doped Alq<sub>3</sub> layer is effective in lowering the driving voltage by reducing the barrier height for the electron injection. In that study, Li donates electrons to the pyridyl ring of Alq<sub>3</sub>, increasing the conductivity of the Alq<sub>3</sub> layer (Kido & Matsumoto, 1998). Recently, Cs-doped Alq<sub>3</sub> films have attracted attention because it is easier for Cs to donate electrons than Li owing to its lower ionization energy. Most work on Cs-doped Alq<sub>3</sub> has been focused on fundamental issues based on the results from the valence band and core-level measurements (Lai *et al.*, 2003; Fung *et al.*, 2004; Ding & Gao, 2005). The major finding relating to the donation of electrons from Cs is the generation of a gap state, reported by Lai *et al.* (2003). Later, Fung *et al.* (2004) and Ding & Gao (2005) further justified the formation of a Cs-induced gap state contributed by electron donation from Cs to nitrogen in the pyridyl ring.

The role of Cs atoms in Cs-doped Alq<sub>3</sub> does not simply result in a chemical shift of core levels. In this article we will present an experimental observation of the bond-cutting of Alq<sub>3</sub> induced by electron donation of Cs in the Cs-doped Alq<sub>3</sub> layer. A series of Cs 4*d* and Al 2*p* core-level spectra, along with valence-band and cut-off spectra, were recorded *in situ* by synchrotron radiation photoemission. With the benefits of strong intensity and surface sensitivity of the technique, bond cutting of Alq<sub>3</sub> by Cs was observed in the Cs-doped Alq<sub>3</sub> layer at high Cs doping concentration.

## 2. Experimental

Mirror-polished *n*-type Si(100) wafers ( $\rho = 1\text{--}10\ \Omega\ \text{cm}$ ) were pre-oxidized using the method of Ishizaka & Shiraki (1986) in order to remove possible carbon contamination. The Si(100) substrates were then mounted on a heating holder inside an ultra-high-vacuum (UHV) photoemission chamber with a base pressure of less than  $7 \times 10^{-11}$  torr. In order to remove the protected oxide layer the Si(100) substrates were annealed stepwise up to 1153 K to obtain a clean Si(001)  $2 \times 1$  surface on which purified Alq<sub>3</sub> powder was vacuum-evaporated. Cs was evaporated from a SEAS getter onto the pre-evaporated Alq<sub>3</sub> layer. The operation pressures for depositing Alq<sub>3</sub> and Cs were maintained below  $1.5 \times 10^{-9}$  and  $5 \times 10^{-10}$  torr, respectively. Photoelectrons were collected with an OMICRON EA125 hemispherical analyzer in the UHV

chamber located at the low-energy spherical-grating monochromator beamline at the National Synchrotron Radiation Research Center in Taiwan.

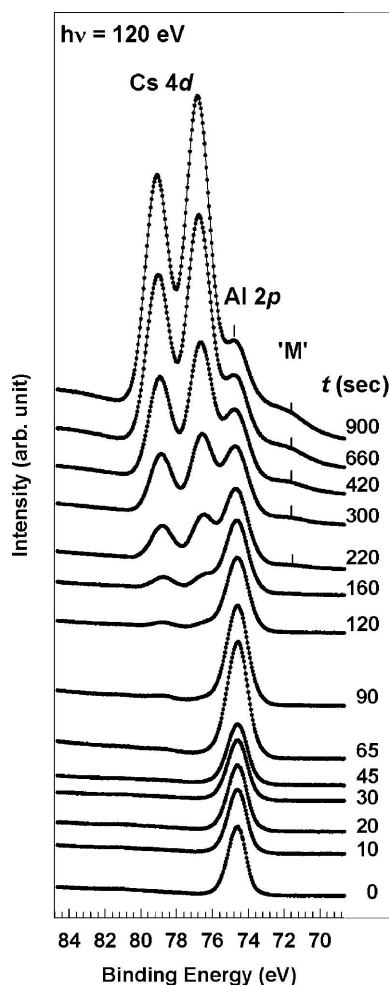
### 3. Results and discussion

The interaction between Cs and Alq<sub>3</sub> was monitored *in situ* using surface-sensitive Al 2*p* and Cs 4*d* core-level spectra (Fig. 1) recorded at a photon energy of 120 eV during deposition of Cs onto a thick Alq<sub>3</sub> layer. The probing depth is estimated to be ~0.5 nm according to the universal curve (Brundle, 1975). The Al 2*p* signal from the pristine Alq<sub>3</sub> is located at a binding energy of 74.6 eV, which appears as a single peak in Alq<sub>3</sub>. As can be seen in Fig. 1, the Al 2*p* signal reduces in intensity with Cs deposition time. No Cs signal was observed at a deposition time of less than 65 s within the detection limit. A very weak Cs 4*d* doublet (4*d*<sub>5/2</sub> and 4*d*<sub>3/2</sub>) begins to appear upon further deposition and gradually becomes the dominant signal above 420 s. In addition to the above-mentioned Cs 4*d* and Al 2*p* signals, a weak signal ('M') also appears at a binding energy of ~71.6 eV at 220 s. The

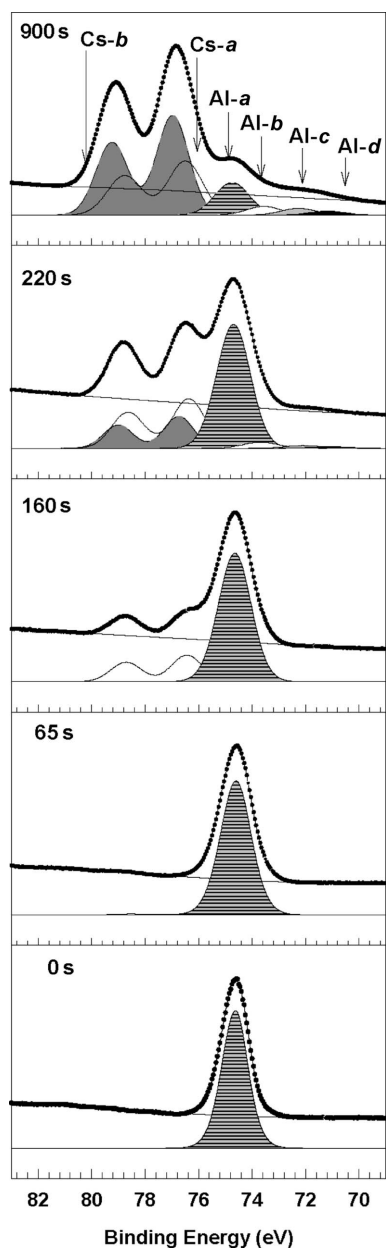
reported binding energy of Al 2*p* in a pure Al metal is 72.7 eV (Gredelj *et al.*, 2001). Based on the energy position, the Cs-induced M state is assigned as the Al 2*p* peak from the metallic Al or a molecule containing Al (Le *et al.*, 2000). The full width at half-maximum of the M state is about 2 eV, which is larger than that of the Al 2*p* in pristine Alq<sub>3</sub> (~1 eV). This suggests that more than one Al-related chemical state is generated owing to the interaction between Cs and Alq<sub>3</sub>. In other words, new types of Al bonds are induced by the doping of Cs into Alq<sub>3</sub>. Examining the molecular structure, it is probable that Cs atoms attach to the O atom in an 8-quinolinoline ligand in Alq<sub>3</sub>, cut the Al–O bonds and form Csq and Alq<sub>2</sub> molecules. The probable chemical reaction is described as Cs + Alq<sub>3</sub> = Csq + Alq<sub>2</sub>. However, the subsequent reaction between Cs and Alq<sub>2</sub> is also possible, which will be discussed later. Note that the later appearance of the M state (220 s) than that of the Cs 4*d* state (65 s) is not due to the cross-section effect since the Al 2*p* core exhibits a higher cross section than the Cs 4*d* core at the present excitation energy (Yeh & Lindau, 1985). The generation of new Al-related chemical states seems to require a critical Cs doping concentration. This implies that a critical Cs concentration is required for the chemical reaction Cs + Alq<sub>3</sub> = Csq + Alq<sub>2</sub> to occur.

Chemical information about the new Al-related chemical states can be extracted through de-convolution of the Cs 4*d* and Al 2*p* core-level spectra in Fig. 1. As shown in Fig. 2, two Cs 4*d* doublets (Cs-*a* and Cs-*b*) and four Al 2*p* peaks (Al-*a*, Al-*b*, Al-*c* and Al-*d*) are required to obtain a consistent fit for all the Cs 4*d* and Al 2*p* spectra. The binding energies of the Cs-*a*, Cs-*b*, Al-*a*, Al-*b*, Al-*c* and Al-*d* components and their corresponding Gaussian widths for all the Cs 4*d* and Al 2*p* spectra are summarized in Table 1. The Al-*a* component at 74.6 ± 0.1 eV arises from the pristine Alq<sub>3</sub>. The binding energy values of Al-*b*, Al-*c* and Al-*d* are 73.5 ± 0.1, 72.1 ± 0.1 and 71.0 ± 0.1 eV, respectively, indicating the existence of three different bonding environments of Al. From a chemical view, Cs reacts rather strongly with the 8-quinolinoline ligands in Alq<sub>3</sub>. Thus, it is possible to disassemble the Alq<sub>3</sub> molecule into Csq and Alq<sub>2</sub> by formation of Csq. Alq<sub>2</sub> is likely to be further dissociated into Alq or even Al in subsequent formations of Csq. Based on the charge transfer between an Al atom and an 8-quinolinoline ligand, the Al atom may donate valence charge towards the O atom in Alq, Alq<sub>2</sub> or Alq<sub>3</sub>. The Al 2*p* component of pure Al is expected to exhibit a binding energy lower than that of Alq, Alq<sub>2</sub> and Alq<sub>3</sub>. Al-*b*, Al-*c* and Al-*d* are thus assigned as the Al 2*p* signals from Alq<sub>2</sub>, Alq and Al, respectively, since the binding energies of Al-*b*, Al-*c* and Al-*d* are in a reduction sequence. Note that the Al 2*p* component of the pure Al atom (71.0 eV) cut out of the Alq<sub>x</sub> molecule, *i.e.* the Al-*d* component, exhibits a binding energy lower than that of pure Al metal (72.7 eV). The energy difference of Al 2*p* is probably due to the different bonding environment between free Al atoms and Al metallic bonds.

The existence of four Al 2*p* components implies that Alq<sub>3</sub> can be bond-cut by the Cs-doped atoms in the Alq<sub>3</sub> layer. Bond cutting of Alq<sub>3</sub> by Cs is also supported by the deconvoluted Cs spectra in Fig. 2, where a new Cs 4*d* doublet begins



**Figure 1**  
Cs 4*d* and Al 2*p* core-level spectra from the Cs/Alq<sub>3</sub> interface at different Cs coverages. The spectra were recorded at a photon energy of 120 eV.


**Figure 2**

Curve fit of the Cs 4d and Al 2p spectra from the Cs/Alq<sub>3</sub> interface at different Cs coverages.

to appear at a deposition time longer than 220 s, concurrently with the appearance of the new Al-related chemical states. Cs-*a* is a state without chemical shift (no charge transfer), which is assigned as the Cs 4d component from the neutral Cs atoms in Alq<sub>3</sub>. Cs-*b* is a state with chemical shift, which is assigned from Csq.

The assignments of the Cs 4d and the Al 2p components in the Cs-doped Alq<sub>3</sub> layer are further justified by their relative amounts at different Cs coverages, as shown in Figs. 3(a) and 3(b). The relative amount of each Cs 4d (or Al 2p) component is expressed as the relative peak area %. The Al-*b*, Al-*c* and Al-*d* components increase in intensity accompanied by an intensity reduction of the Al-*a* component at deposition times

**Table 1**

Relative binding energies of the Cs 4d<sub>5/2</sub> and Al 2p<sub>3/2</sub> components and their corresponding Gaussian widths.

Average values of binding energy and Gaussian width with error margin for each component are also listed.

	Coverage (s)	Binding energy (eV)	Gaussian width (eV)	Area percentage (%)
Cs- <i>a</i>	65	76.3	1.32	100
	160	76.4	1.35	100
	220	76.4	1.45	63.2
	300	76.3	1.45	49.9
	420	76.4	1.51	41.7
	660	76.4	1.53	39.2
	900	76.5	1.54	36.8
		Average 76.4 ± 0.1	Average 1.45 ± 0.13	
Cs- <i>b</i>	220	76.7	1.45	36.8
	300	76.8	1.45	50.1
	420	76.8	1.50	58.3
	660	76.9	1.53	60.8
	900	77.0	1.54	63.2
			Average 76.8 ± 0.2	Average 1.49 ± 0.05
Al- <i>a</i>	0	74.5	1.05	100
	65	74.5	1.29	100
	160	74.5	1.39	100
	220	74.6	1.44	92.0
	300	74.6	1.42	85.2
	420	74.6	1.45	79.5
	660	74.6	1.43	69.4
	900	74.6	1.43	62.8
		Average 74.6 ± 0.1	Average 1.36 ± 0.31	
Al- <i>b</i>	220	73.5	1.46	4.6
	300	73.6	1.44	7.5
	420	73.5	1.45	10.0
	660	73.4	1.42	13.3
	900	73.4	1.42	16.6
			Average 73.5 ± 0.1	Average 1.44 ± 0.02
Al- <i>c</i>	220	72.0	1.46	2.1
	300	72.0	1.47	5.0
	420	72.1	1.45	7.1
	660	72.1	1.46	11.3
	900	72.1	1.43	13.0
			Average 72.1 ± 0.1	Average 1.45 ± 0.02
Al- <i>d</i>	220	71.0	1.43	1.2
	300	71.0	1.47	2.2
	420	70.9	1.45	3.4
	660	70.9	1.42	6.0
	900	71.1	1.44	7.6
			Average 71.0 ± 0.1	Average 1.44 ± 0.03

longer than 220 s. This implies that the Al-*a* component is from the pristine Alq<sub>3</sub> and that the Al-*b*, Al-*c* and Al-*d* components are from the induced Al-related chemical states. Note that the closer the component is to the Al-*a* component the greater the increase in intensity. The Al-*b* component is thus assigned as the decomposed Alq<sub>2</sub> molecule since it exhibits a highest peak area among the induced components. As for the Al-*c* and Al-*d* components, we assign them as the Alq molecule and the free Al atom, respectively. Note that Cs-*a* decreases and Cs-*b* increases at deposition times longer than 220 s. This supports the assignment of Cs-*b* as Csq since the generation of Csq is expected to increase with Cs doping concentration. Cs-*a* is assigned from the neutral Cs atoms in Alq<sub>3</sub>, since some Cs atoms are consumed to react with Alq<sub>3</sub> in favor of Csq formation and result in the peak area reduction of Cs-*a*.

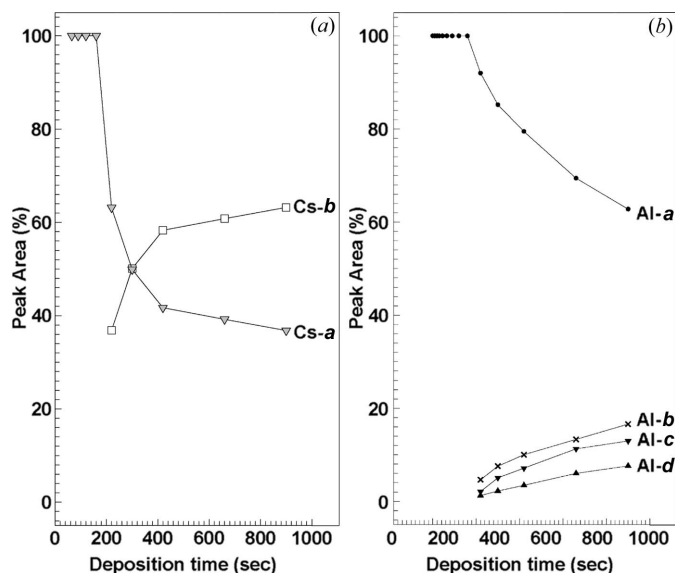


**Figure 3** Relative amounts of each component of Cs and Al core levels for different Cs coverages: (a) Cs 4d and (b) Al 2p. The relative amount of each component is expressed as peak area %.

Fig. 4(a) shows the surface-sensitive valence band spectra of Alq<sub>3</sub> doped with different Cs coverages, recorded *in situ* at a photon energy of 46 eV. The peaks A–G are the characteristic peaks for Alq<sub>3</sub>, which reduce in intensity with Cs doping (Ishii & Seki, 1997; Sugiyama *et al.*, 1998). No Fermi edge was observed, even at 900 s (the highest Cs doping in our study), indicating that no metallic Cs exists at the Cs/Alq<sub>3</sub> interface. The highest occupied molecular orbital (HOMO) peak ‘A’ stays at ~3 eV at a deposition time less than 65 s, but gradually shifts towards higher binding energy and reaches ~4 eV at 220 s. The HOMO peak continues to shift towards higher binding energy at 65–220 s, which is before the bond cutting at 220 s. Similar to surface band bending, some extent of charge may be donated from Cs to Alq<sub>3</sub> near the surface to form a dipole layer, which causes the downward HOMO peak shift. Note that the HOMO peak remains at the same position at deposition times longer than 400 s.

The shift of the HOMO peak is consistent with the energy shift of the cut-off at different Cs coverages, as shown in Fig. 4(b). The cut-off shifts to higher binding energy, which indicates a downward bending of the vacuum level owing to the doping of Cs. The downward bending is attributed to the ‘donor’ character of Cs atoms in Alq<sub>3</sub>. The charge donation from Cs may result in an effective dipole layer near the Cs/Alq<sub>3</sub> interface and cause the downward bending and the downward HOMO peak shift.

In summary, Cs is very reactive with Alq<sub>3</sub>; however, a critical concentration exists below which no chemical reaction occurs. At a concentration lower than the critical one, Cs atoms may donate electrons to Alq<sub>3</sub> near the surface and cause downward bending of the cut-off and the HOMO peak. At a concentration higher than the critical one, bond cutting of Alq<sub>3</sub> by Cs occurs. An Alq<sub>3</sub> molecule may be disassembled into

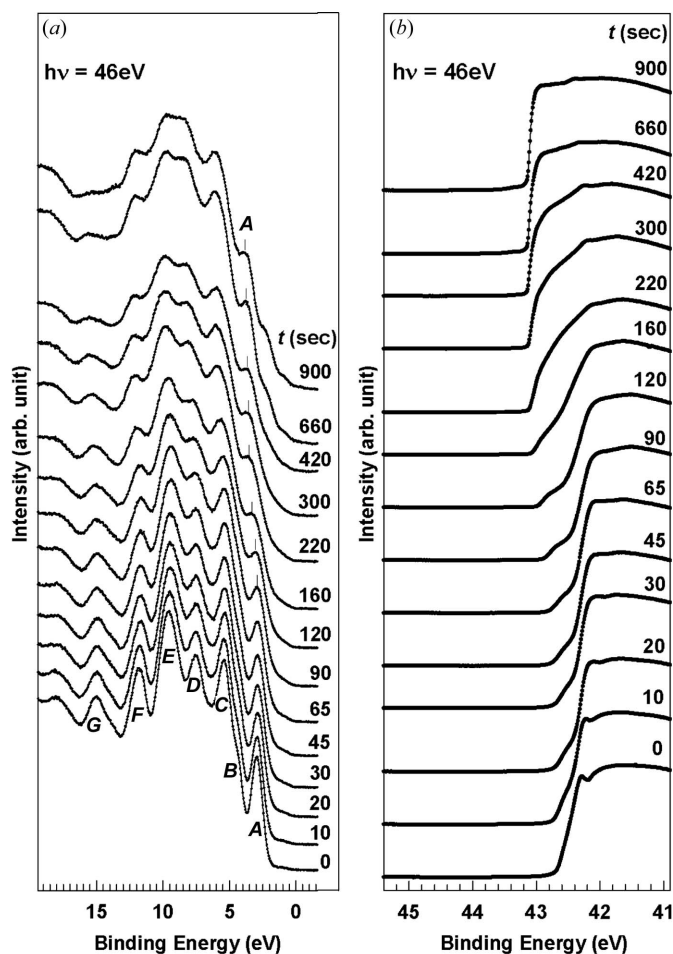


**Figure 4** (a) Surface-sensitive valence-band spectra from the Cs/Alq<sub>3</sub> interface at different Cs coverages. (b) Cut-off spectra from the Cs/Alq<sub>3</sub> interface at different Cs coverages. The spectra were recorded at a photon energy of 46 eV.

Csq and Alq<sub>2</sub> by formation of Csq through a bond-cutting mechanism. Subsequent formations of Alq and Al are also possible by bond cutting of Alq<sub>2</sub> and Alq by Cs.

The work is sponsored by the National Science Council through project NSC 95-2112-M-213-001.

### References

Brundle, C. R. (1975). *Surf. Sci.* **48**, 99–136.  
 Ding, H. & Gao, Y. (2005). *Appl. Phys. Lett.* **86**, 213508.  
 Fung, M. K., Lai, S. L., Tong, S. W., Bao, S. N., Lee, C. S. & Lee, S. T. (2004). *Chem. Phys. Lett.* **392**, 40–43.  
 Gredelj, S., Gerson, A. R., Kumar, S. & Cavallaro, G. P. (2001). *Appl. Surf. Sci.* **174**, 240–250.  
 Haskal, E. I., Curioni, A., Seidler, P. F. & Andreoni, W. (1997). *Appl. Phys. Lett.* **71**, 1151–1153.  
 Ishii, H. & Seki, K. (1997). *IEEE Trans. Electron Devices*, **44**, 1295–1301.  
 Ishizaka, A. & Shiraki, Y. (1986). *J. Electrochem. Soc.* **133**, 666–671.

- Kido, J. & Matsumoto, T. (1998). *Appl. Phys. Lett.* **73**, 2866–2868.
- Kido, J., Nagai, K. & Okamoto, Y. (1993). *IEEE Trans. Electron Devices*, **40**, 1342–1344.
- Lai, S. L., Fung, M. K., Bao, S. N., Tong, S. W., Chan, M. Y., Lee, C. S. & Lee, S. T. (2003). *Chem. Phys. Lett.* **367**, 753–758.
- Le, Q. T., Yan, L., Gao, Y., Mason, M. G., Giesen, D. J. & Tang, C. W. (2000). *J. Appl. Phys.* **87**, 375–379.
- Shi, J. & Tang, C. W. (1997). *Appl. Phys. Lett.* **70**, 1665–1667.
- Sugiyama, K., Yoshimura, D., Miyamae, T., Miyazaki, T., Ishii, H., Ouchi, Y. & Seki, K. (1998). *J. Appl. Phys.* **83**, 4928–4938.
- Tang, C. W., VanSlyke, S. A. & Chen, C. H. (1989). *J. Appl. Phys.* **65**, 3610–3616.
- Yeh, J. J. & Lindau, I. (1985). *Atom. Data Nucl. Data Tables*, **32**, 1–155.